Formation of Micelles of Diblock and Triblock Copolymers in a Selective Solvent

D. Izzo[†] and C. M. Marques[*,‡]

Institut Charles Sadron, 6 rue Boussingault, 67083 Strasbourg Cedex, France, and Instituto de Física da Universidade de São Paulo, Caixa Postal 20 516, 01498 São Paulo, Brazil

Received May 6, 1993; Revised Manuscript Received September 24, 1993[•]

ABSTRACT: We study theoretically the formation of dilute phases of spherical (micelles), cylindrical (vermicelles), and planar (lamellae) aggregates of copolymer chains in a selective solvent. In the case of diblock copolymer chains, micelles are formed for all values of the block asymmetry in the regime where dilute phases are predicted to occur ($N_A \ll N_B^{3/2}$, with N_A and N_B the polymerization indices of the A-collapsed and B-swollen blocks). For B–A–B triblock copolymers we find that spherical or cylindrical hollow structures might exist in the solvent in a metastable state with a long associated lifetime.

I. Introduction

Diblock copolymer chains in a selective solvent are the macromolecular analogs of low molecular weight surfactants. The nonsoluble A-block of the copolymer chain adopts a collapsed configuration, while the B-block is well swollen by the solvent. By assembling with other chains in a variety of geometries (spherical, cylindrical, planar, etc.), the collapsed blocks minimize contact with the solvent and thus reduce the enthalpy of the system. However, for entropic reasons, aggregation only occurs at finite-chain concentration: at very low concentrations only isolated chains are present in the solution.[1] The exact geometry of the aggregates depends primarily on the relative sizes of each of their blocks. It is, for instance, well established that chains with a small collapsed block adopt a spherical configuration, forming spherical micelles with a dense molten core and a hairy corona,[2] but little is known for diblock copolymers with arbitrary asymmetry, i.e., chemical composition. In the next section we investigate the possibility of the formation of dilute phases of spherical (micelles), cylindrical (vermicelles), or planar (lamellae) aggregates of diblock copolymer chains. In section III we study the aggregation of triblock copolymers in a selective solvent. The triblock copolymers considered here have a nonsoluble middle A-block and two soluble B-blocks at both extremities of the chains. The main motivation for studying these types of polymers is that they are good candidates for the formation of hollow structures where the collapsed blocks form a molten spherical or cylindrical skin protected on both sides by two coronas of well-swollen polymers. In the last section we discuss the experimental relevance of our predictions.

II. Polymer Structures in Solution

In this section we compare the relative stability of three possible structures: spherical (micelles), cylindrical (vermicelles), and planar (lamellae). Let c_1 be the number density of free chains in solution, while $c_s(p)$, $c_c(p)$, and $c_l(p)$ stand for the number density of spherical, cylindrical, and planar aggregates of p chains. Since we expect the aggregation process to occur at low concentrations, the free-energy density of the solution can be written as

$$F = c_1[\log c_1 + F_1] + \sum_{p=2}^{\infty} c_s[\log c_s + F_s(p)] + \sum_{p=2}^{\infty} c_c[\log c_c + F_c(p)] + \sum_{p=2}^{\infty} c_l[\log c_l + F_l(p)] \quad \text{(II.1)}$$

where $F_i(p)$ (i = s, c, l) are the free energies of several aggregates and F_1 is the free energy of the single chains. All free energies are measured in units where $K_BT = 1$. The corresponding concentrations can be found by minimizing the free-energy density under the constraint of conservation of the total number of chains ϕ

$$c_1 + \sum_{p=2}^{\infty} p[c_s(p) + c_c(p) + c_l(p)] = \phi \quad \text{(II.2)}$$

leading to

$$c_1 = \exp\{-F_1 - 1 + \mu\}; \quad c_i(p) = \exp\{-F_i(p) - 1 + \mu p\}, \quad i = \text{s, c, l} \quad \text{(II.3)}$$

where μ is a Lagrange multiplier (or chemical potential) that ensures conservation of the total number of chains. The conservation constraint (eq II.2) can be rewritten as

$$1 + \sum_{p=2}^{\infty} p[\exp\{-\Omega_s(p)\} + \exp\{-\Omega_c(p)\} + \exp\{-\Omega_l(p)\}] = \exp\{F_1 + 1 + \ln \phi - \mu\} \quad \text{(II.4)}$$

where $\Omega_i(p)$ (i = s, c, l) are the grand potentials defined by $\Omega_i(p) = F_i(p) - F_1 - \mu(p-1)$. Equation II.2 shows that, for very low concentrations where the grand potentials Ω_i are strongly positive everywhere, the chemical potential μ can be expressed as

$$\mu = \ln \phi + F_1 + 1 \quad \text{(II.5)}$$

The chemical potential is thus an increasing function of the concentration, taking negative values for very low concentrations. Equation II.5 ceases to be valid whenever one of the grand potentials Ω_j starts to contribute strongly to the conservation equation (eq II.4). At this point aggregates of the type j will be formed in the solution, determining the value of the chemical potential. However, the criteria which determines how strongly the grand potentials contribute to the conservation equation depend on the exact form of these potentials. It is thus instructive

[†] Instituto de Física da Universidade de São Paulo.
[‡] Institute Charles Sadron.
[•] Abstract published in *Advance ACS Abstracts*, November 15, 1993.

0024-9297/93/2226-7189$04.00/0

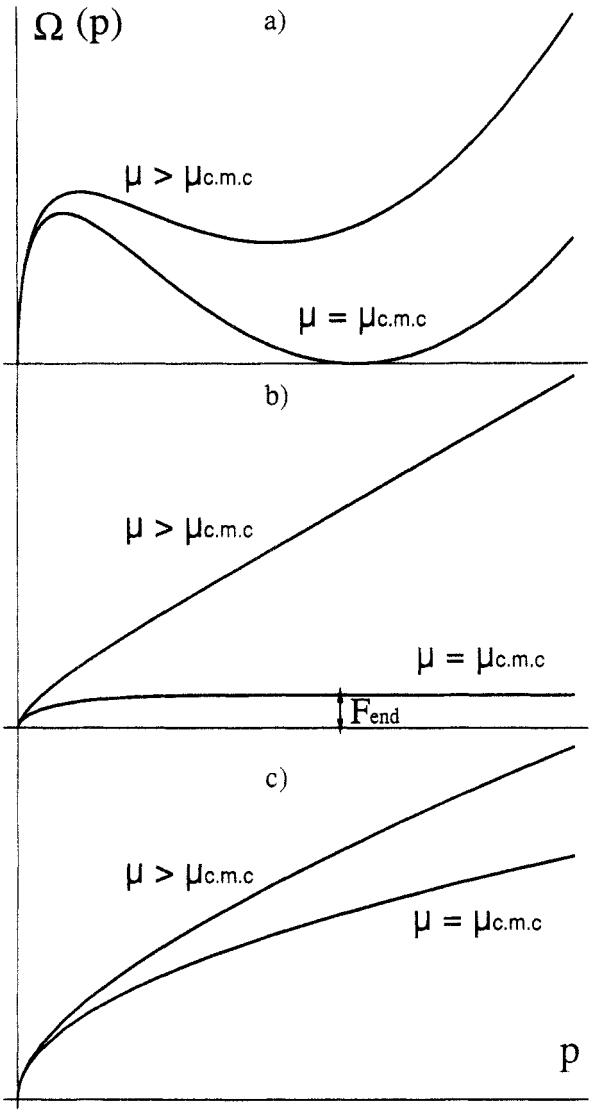

Figure 1. Grand potential Ω as a function of aggregation number p: (a) micelles; (b) vermicelles; (c) lamellae.

first to consider independently the formation of each structure. We sketch in Figure 1 the typical shapes of the grand potentials for different values of μ.

In the case of micelles the grand potential $\Omega_s(p)$ has a minimum at an aggregation number p larger than unity. At some value of the chemical potential μ_{cmc} (and therefore of the concentration) the minimum of Ω_s at $p = p_{cmc}$ tends asymptotically to zero, largely contributing to the sum on the left-hand side of eq II.4. At this point (usually known as the critical micellar concentration, cmc) a finite (large) number of micelles of size close to p_{cmc} is to be observed in the solution, and any increase in concentration will not affect the value of the chemical potential which is bound by μ_{cmc}. The polydispersity of aggregation numbers around p_{cmc}, which turns out to be extremely small for all the spherical cases considered below, is related to the curvature of the potential at the minimum and can be calculated from[3] $\Delta p = (\partial^2\Omega/\partial p^2)^{-1/2}$.

For the cylindrical structures there is no minimum in the grand potential. For large aggregation numbers, the potential is a linear function of p, $\Omega_c \simeq (F_{min} - \mu)p + F_{end}$; F_{min} is the free energy of a chain inside the cylinder, and F_{end} accounts for the difference in free energy for the chains at the end caps of the cylinders. The corresponding size distribution is exponential with associated average size $\bar{p} = (F_{min} - \mu)^{-1}$. As the slope $F_{min} - \mu$ vanishes, the average aggregation number of the cylinders diverges. At this point, the conservation equation fixes the chemical potential to the value $\mu = F_{min} - \phi^{-1/2} \exp\{-(F_{end} + 1)/2\}$. As the concentration increases, the chemical potential approaches the upper bound F_{min} fixed by the geometry of the aggregates. The micellization (we should say, the vermicellization) for cylinders is thus qualitatively different from the micellization for spheres. In the case of micelles, aggregates with a well-defined aggregation number will be formed at the cmc. In the case of cylinders, the aggregates slowly grow from the solution with a broad distribution of aggregation numbers.

The formation of planar structures is rather different from the two precedent cases. A simple picture for the appearance of lamellae of aggregation number p would be provided by considering the formation of disks of finite size. The corresponding grand potential would have the asymptotic form $\Omega_l \simeq (F_{min} - \mu)p + F_{edge}p^{1/2}$. Similar to the cylindrical case, the main contribution to the free energy is linear in p. However, because of the two-dimensional geometry, the contribution to the energy from the chains on the edge of the disks is p dependent. This implies that no finite amount of disks can be present in the solution for $\mu \leq F_{min}$. For $\mu > F_{min}$ the number of aggregates with large p values diverges, suggesting a phase separation between a dilute solution of isolated chains and a dense lamellar phase. The usual conditions for thermodynamic equilibrium read

$$\begin{cases} \mu_A = \mu_B \\ F_A(\phi_A) = F_B(\phi_B) + \mu_A(\phi_A - \phi_B) \end{cases} \quad \text{(II.6)}$$

where μ_A, μ_B, F_A, F_B, ϕ_A, and ϕ_B are respectively the chemical potentials, free energies, and chain volume fractions in the dilute (A) and lamellar (B) phases. Equation II.6 determines the chain volume fractions of the two phases. The relative amount of volume occupied by the lamellar phase X is then simply given by $X = (\phi - \phi_A)/(\phi_B - \phi_A)$.

The aggregation process can thus be studied as follows. For a given structure we write the grand canonical function and determine the upper bound for the chemical potential, μ_α (α = cmc, cvc, and clc). The stable structure to be formed at chain concentration ϕ_α is roughly given by

$$\ln \phi_\alpha = \mu_\alpha - F_1 - 1 \quad \text{(II.7)}$$

where α is the structure corresponding to the smallest critical chemical potential. We proceed by studying the micellization of diblock copolymer chains and then the micellization of triblock copolymers.

III. Self-Assembly of Diblock Copolymers in a Selective Solvent

We consider a solution of diblock copolymer chains of type A–B. The nonsoluble A-block has degree of polymerization N_A and adopts a collapsed configuration, occupying a volume $V = N_A a^3$, where a is the monomer size. Hereafter, we choose length units where $a = 1$. Blocks B are well swollen by the solvent and have degree of polymerization N_B. For all the geometries considered there are three main contributions to the free energy: the elastic deformation of the A chains in the molten part, the corona osmotic energy, and the interfacial tension betwen the A part and the solvent. We anticipate that, depending on the relative values of the polymerization indexes N_A and N_B, it is possible to define three different regimes:

I. *The star regime* ($N_A \ll N_B^{15/11}$). In this regime[4,5] the size of the external corona of micelles and verimicelles is much larger than the core size, and the osmotic contri-

bution from the corona largely dominates the elastic contribution from the chains in the core.

II. *The intermediate regime* ($N_B^{15/11} \ll N_A \ll N_B^{18/11}$). Here the size of the external corona of micelles and vermicelles is much smaller than the core size, but the osmotic contribution from the corona is still much larger than the elastic contribution from the chains in the core.

III. *The ball regime* ($N_B^{18/11} \ll N_A$). This corresponds to the regime where the size of the external corona of micelles and verimicelles is much smaller than the core size, and the elastic contribution from the chains in the core is much larger than the corona osmotic contribution.

One may wonder at this point what is the maximum asymmetry of the diblock copolymers which still allows for solvency of the whole chain. If one considers single isolated chains, an upper bound asymmetry is simply given by comparing the reference chemical potentials of the well-solvated part (which is proportional to N_B) and of the collapsed block which gives a contribution proportional to $N_A^{2/3}$. This leads to an upper bound for the existence of dilute phases at $N_A = N_B^{3/2} = N_B^{16.5/11}$, located at the center of the intermediate regime. However, the ball regime still needs to be considered because aggregates have a higher solvency than single chains. For instance, for micelles in the ball regime, the typical aggregation number is on the order of N_A, shifting the upper solvency bound to much larger asymmetries ($N_A \ll N_B^{30/11}$). A complete discussion of the solvency effects needs to be postponed until the relative stability of the three phases has been established. We will return to this point in the final discussion of section III. Next we describe the different structures in each of the three regimes.

III.1. Spherical Structures. The spherical micelles have a dense spherical core of radius $R_A = (3/(4\pi)pN_A)^{1/3}$ and a corona of size R_B. In the *star regime*, a geometry first described by Daoud and Cotton,[4] the corona is much larger than the core radius, and one has $R_B \sim N_B^{3/5}p^{1/5}$. The free-energy contribution from the corona can be written as $F_{corona} = Ap^{3/2}$, where A is a constant of order unity. The grand potential $\Omega_s(p)$ reads

$$\Omega_s = A(p^{3/2} - 1) + 4\pi\gamma[R_A^2(4p) - R_A^2(1)] - \mu(p - 1) \tag{III.1}$$

In the following we use the core radius R_A as the running variable and adopt renormalized quantities: $\tilde{\mu} = \mu N_A^{-2/5}\gamma^{-3/5}$, $r = R_A N_A^{3/5}\gamma^{-2/5}$, and $\tilde{\Omega}_s = \Omega_s N_A^{-6/5}\gamma^{-9/5}$. In these unities the different quantities to be calculated at the cmc reduce to an ensemble of numerical values (up to N_A dependent corrections of order $N_A^{-4/5}$, that we shall systematically neglect). These numerical values can be readily calculated from eq II.7), by imposing $d\tilde{\Omega}/dr = \tilde{\Omega} = 0$. This leads to

$$\begin{cases} \tilde{\mu}_{cmc} = 5(\pi A^2/3)^{1/5} \\ r_{cmc} = (\pi A^2/3)^{-1/5} \end{cases} \tag{III.2}$$

In the *intermediate regime* the radius of the corona is much smaller than the core radius. The corona has thus the structure of a brush, and the dominant contribution to the free energy is of the form $F_{corona} = 4\pi R_A^2 B N_B \sigma^{11/6}$, where B is a constant of order unity and σ is the density of chain ends $\sigma = p/(4\pi R_A^2)$. The grand potential can be written as (up to $O(N_A^{-1})$ corrections):

$$\tilde{\Omega}_s = \frac{4\pi B}{3^{11/6}} r^{23/6} + 4\pi r^2 - \tilde{\mu}\frac{4\pi}{3} r^3 \tag{III.3}$$

where the reduced variables are $\tilde{\mu} = \mu N_B^{-6/11}\gamma^{-5/11}$, $r = R_A N_B^{6/11} N_A^{-1}\gamma^{-6/11}$, and $\tilde{\Omega}_s = \Omega_S N_B^{12/11} N_A^{-2}\gamma^{-23/11}$. At the cmc these variables assume the following numerical values

$$\begin{cases} \tilde{\mu}_{cmc} = (11/5)(5B/6)^{6/11} \\ r_{cmc} = 3(5B/6)^{-6/11} \end{cases} \tag{III.4}$$

In the *ball regime* the elastic energy of the polymers in the core of the micelle is much larger than the contribution from the corona. Because the chains in the core are grafted to a convex surface, it is possible to compute exactly the free energy. Following ref 6, we write

$$\tilde{\Omega}_s = \frac{\pi^3}{60} r^5 + 4\pi r^2 - \mu\frac{4\pi}{3} r^3 \tag{III.5}$$

with $\tilde{\mu} = \mu N_A^{-1/3}\gamma^{-2/3}$, $r = R_A N_A^{-2/3}\gamma^{-1/3}$, and $\tilde{\Omega}_s = \Omega_s N_A^{-4/3}\gamma^{-5/3}$. At the cmc we have

$$\begin{cases} \tilde{\mu}_{cmc} = (9/4)(\pi^2/15)^{1/3} \\ r_{cmc} = 2(\pi^2/15)^{-1/3} \end{cases} \tag{III.6}$$

III.2. Cylindrical Structures. In order to compute the critical vermicellar concentration, we consider infinite cylindrical aggregates; that is, we neglect end-cap effects which are only important to determine the average mass distribution. The chains are packed along the cylinder with density $D^{-1} = \pi R_A^2/N_A$. In the *star regime* the radius of the corona scales as $R_B \sim N_B^{3/4}D^{-1/4}$, and the free energy per chain is $F_{corona} = CN_B^{3/8}D^{-5/8}$, with C and D being constants of order unity. The grand potential reads

$$\frac{\tilde{\Omega}_c}{p} = C\pi^{5/8} r^2 + \frac{2}{r} - \tilde{\mu} \tag{III.7}$$

The renormalized variables are $r = R_A N_A^{-13/18} N_B^{1/6}\gamma^{-4/9}$ and $\tilde{\mu} = \mu N_A^{-5/18} N_B^{-1/6}\gamma^{-5/9}$. The renormalization of $\tilde{\Omega}/p$ is identical to that of $\tilde{\mu}$. At the cvc we have

$$\begin{cases} \tilde{\mu}_{cvc} = (18/5)(5C\pi^{5/8}/8)^{4/9} \\ r_{cvc} = (5C\pi^{5/8}/8)^{-4/9} \end{cases} \tag{III.8}$$

In the *intermediate regime* the corona radius is much smaller than the core radius but still dominates the contribution to the free energy, which is of the form $F_B = BN_B\sigma^{11/6}$, where B is the same numerical constant which appears in the first term on the right-hand side of eq III.3 and the end density is now given by $\sigma = (2\pi R_A D)^{-1}$. The grand potential can be written as

$$\frac{\tilde{\Omega}_c}{p} = \frac{B}{2^{5/6}} r^{5/6} + \frac{2}{r} - \tilde{\mu} \tag{III.9}$$

and the various quantities are renormalized as in the intermediate case of the spherical structures. Evaluating the values of the coefficients at the cvc, one obtains

$$\begin{cases} \tilde{\mu}_{cvc} = (11/5)(5B/6)^{6/11} \\ r_{cvc} = 2(5B/6)^{-6/11} \end{cases} \tag{III.10}$$

For the *ball regime*, where the elastic energy of the core dominates, one has[6]

$$\frac{\tilde{\Omega}_s}{p} = \frac{\pi^3}{48} r^2 + \frac{2}{r} - \tilde{\mu} \tag{III.11}$$

with renormalized parameters as in the ball regime of micelles. At the cvc we have

$$\begin{cases} \tilde{\mu} = 3(\pi^2/48)^{1/3} \\ r = (\pi^2/48)^{-1/3} \end{cases} \tag{III.12}$$

III.3. Planar Structures. For the lamellae we also consider infinite isolated sheets of associated diblocks, as

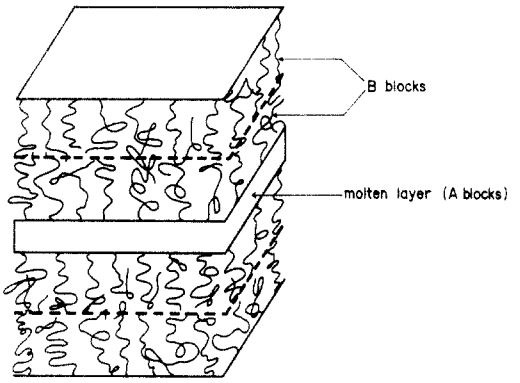

Figure 2. Isolated (infinite) sheet in the lamellar structure.

sketched in Figure 2. It can be consistently checked *a posteriori* that such isolated sheets are responsible for the leading contributions to the energy of the local planar structure of the dense lamellar phase. The main neglected term is the van der Waals interaction[7] which ensures the adhesion of adjacent bilayers; effectively, this interaction does not affect the equilibrium structure features, amounting only to a small reduction of the interfacial tension coefficient γ. Note also that steric interactions[8] of fluctuating nature (Helfrich interactions) can be neglected in polymeric planar structures, because of the high bending moduli of the layers. Because the curvature radius is infinite, there are only two regimes for the lamellae: the intermediate and the ball regimes. The first one is described by a grand potential of the form

$$\frac{\tilde{\Omega}_c}{p} = Br^{5/6} + \frac{1}{r} - \tilde{\mu} \qquad \text{(III.13)}$$

with renormalized parameters as in the intermediate cases of the spherical and cyclindrical geometries. At the critical lamellar concentration we have

$$\begin{cases} \tilde{\mu}_{clc} = (11/5)(5B/6)^{6/11} \\ r_{clc} = (5B/6)^{-6/11} \end{cases} \qquad \text{(III.14)}$$

The *ball regime* (where the elastic energy from the molten layer is dominant) is described by

$$\frac{\tilde{\Omega}_s}{p} = \frac{\pi^3}{24}r^2 + \frac{1}{r} - \tilde{\mu} \qquad \text{(III.15)}$$

with a renormalization identical to the ball regimes of the precedent geometries. At the clc one has

$$\begin{cases} \tilde{\mu} = (1/2)(3\pi^2/2)^{2/3} \\ r = (12/\pi^2)^{1/3} \end{cases} \qquad \text{(III.16)}$$

III.4. Discussion. We can discuss the formation of the different structures by comparing the respective chemical potentials of each of the regimes considered. In the *star regime* ($N_A \ll N_B^{15/11}$), where the dimension of the collapsed blocks is much shorter than the dimension of the swollen blocks, it is clear that the preferred structures are the spherical micelles (compare eqs III.2, III.8, and III.14). On the other hand, in the *ball regime* ($N_A \gg N_B^{18/11}$), where the diblock copolymers have a collapsed block much larger than the swollen block, the lamellar dense phase always has a chemical potential lower than the two other phases (eqs III.6, III.12, and III.16).

In the *intermediate regime* ($N_B^{15/11} \ll N_A \ll N_B^{18/11}$), the critical chemical potentials of the three phases have the same value (eqs III.4, III.10, and III.14). In order to decide which phase is preferred in this regime, one needs to take into account the leading corrections[7] to the grand potentials: the elastic energies of the core and the curvature corrections of the brush in the corona (note that since the areal density of B chains on the surface of the A cores is the same for the three structures, the entropy associated with the A–B junction points is not a relevant correction to the free energy). Because these contributions are small, the shift in the critical chemical potentials can be calculated perturbatively. This shift is given by the contribution of the additional free energy per chain, evaluated with the parameters calculated above from the main (noncorrected) contributions to the grand potentials. The elastic energy corrections can be computed from the expressions of the ball regime. The chemical potential shift $\Delta\mu$ associated to the elastic corrections is

$$\begin{cases} \Delta\mu_{cmc} = 9\pi^2/80(5A/6)^{-12/11}N_A N_B^{12/11} \\ \Delta\mu_{cvc} = 20/27\Delta\mu_{cmc} \\ \Delta\mu_{clc} = 10/27\Delta\mu_{cmc} \end{cases} \qquad \text{(III.17)}$$

The spontaneous curvature corrections are given by the first term in the expansion of the brush free energy in powers of the radius of curvature. These corrections lead to the following shifts in the chemical potential

$$\begin{cases} \Delta\mu_{cmc} = -2C_1 N_B^2 \sigma^{7/6}/R_A = -2C_1/3(5B/6)^{-1/11}N_B^{21/11}N_A^{-1} \\ \Delta\mu_{cvc} = -C_1 N_B^2 \sigma^{7/6}/R_A = 3/4\Delta\mu_{cmc} \end{cases} \qquad \text{(III.18)}$$

where σ is the density of junction points and C_1 is a numerical constant of order unity. Note that, by symmetry, there is no spontaneous curvature correction to the lamellar structure where the chains are packed in bilayers. The minus signs in the corrections to the chemical potential show that, for the same junction point densities, the chains in the curved corona are less stretched than those in the corresponding planar structure.

Equations III.17 and III.18 show that for asymmetries where the curvature corrections are dominant ($N_B^{15/11} \ll N_A \ll N_B^{16.5/11}$), the spherical structures are preferred. On the other hand, for asymmetries where the elastic contribution is the leading corrective term ($N_B^{16.5/11} \ll N_A \ll N_B^{18/11}$), the lamellar structure is preferred.

Our approach leads to the conclusion that there is no value of asymmetry for which vermicelles are the thermodynamically stable aggregates. When the chemical composition (asymmetry) is in the range $N_A \ll N_B^{3/2}$, only micelles are predicted to form. Above this threshold, the lamellar phase has the lowest critical chemical potential of the three phases, ruling out the possibility of dilute phases of micelles or vermicelles with a large collapsed core. It is interesting to note that the critical value of the asymmetry which has been obtained here (by comparing the relative magnitudes of the elastic and spontaneous curvature corrections in the intermediate regime) coincides with the simple arguments invoked before when one studied the solubility of single chains in solution. This leads to a simple picture of micelle formation: for asymmetries such that solvency of single chains is verified ($N_A \ll N_B^{3/2}$), spherical micelles are formed in the solution, while for larger asymmetries, a dense phase is formed. We have only studied the formation of a lamellar dense phase. However, other mesophases should be considered, for instance, the formation of hexagonal or cubic mesophases with a liquid core of well swollen small B chains and a majority molten phase of the A blocks. We will address this issue in a forthcoming paper.

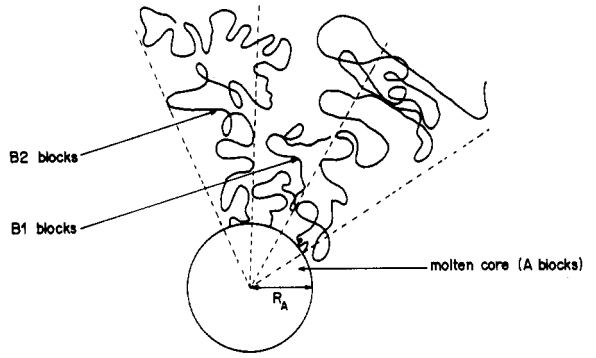

Figure 3. Geometry of the compact core structure in the case of triblock copolymers. We show the case of a micelle with generic asymmetry.

IV. Self-Assembly of Triblock Copolymers in a Selective Solvent

We consider in this section the formation of micelles, vermicelles, and lamellae from dilute solutions of triblock copolymers of the type B–A–B. The nonsoluble A-block has degree of polymerization N_A and adopts a collapsed configuration. Blocks B are well swollen by the solvent and have degrees of polymerization N_{B1} and N_{B2}. In addition to the three structures studied in the case of diblock copolymers, in the triblock copolymer case there is a new interesting possibility to be considered: the formation of hollow structures where the collapsed blocks form a molten spherical or cylindrical skin carpeted on both sides by a brush of the B blocks. Note that there are at least two important differences between the case of asymmetric triblocks and mixtures of diblock copolymers with $N_A/2$'s but with different N_B's. The first is that the relative composition of large and small chains is fixed at half. The other differences is the impossibility for the triblocks to laterally phase separate between smaller and larger chains. We expect thus the behavior of asymmetric triblocks to be somewhat simpler than the behavior of diblock mixtures. In the following we start by studying structures with a compact core formed by the triblocks and then analyze the hollow structures.

IV.1. Aggregates with a Compact Core. We sketched in Figure 3 the geometry of the compact core structures for triblock copolymers. The geometry of the core is quite similar to that of the diblock chains, except that in the present situation the two ends of the A blocks are bound to lie at the interface between the collapsed chains and the solvent. The core can thus be regarded as composed of twice as many chains, each of them having degree of polymerization $N_A/2$. In the *ball regime*, where the contribution from the external corona is not important, this similarity results in a very simple rule to derive the critical chemical potentials for triblock copolymers from the results obtained in the diblock case:

$$\mu_\alpha^{tri} = 2\mu_\alpha^{di}(N_A/2) = 2^{2/3}\mu_\alpha^{di}; \quad \alpha = \text{cmc, cvc, clc} \qquad \text{(IV.1)}$$

In the *intermediate regime*, where both N_{B1} and N_{B2} obey the inequality $N_{Bi}^{15/11} \ll N_A \ll N_{Bi}^{18/11}$ ($i = 1, 2$), the corona can be viewed as a bidisperse brush.[9] We take without loss of generality $N_{B1} < N_{B2}$. The free-energy density for the polydisperse brush can be written as $F = B[N_{B1}(2\sigma)^{11/16} + (N_{B2} - N_{B1})\sigma^{11/6}]$, and the resulting grand potential for the spherical structures is

$$\tilde{\Omega}_s = \frac{4\pi B}{3^{11/6}} r^{23/6}[1 + \rho(2^{11/6} - 1)] + 4\pi r^2 - \tilde{\mu}\frac{4\pi}{3} r^3 \qquad \text{(IV.2)}$$

where we defined $\rho = N_{B1}/N_{B2} \le 1$. By comparing eqs III.3 and IV.2, it can been seen that all the results from the diblock copolymers are readily transposable to the triblock case by replacing the constant B by an effective constant $B[1 + \rho(2^{1/6} - 1)]$. It can be easily checked that this replacement also holds for the other structures, leading to the critical chemical potentials

$$\mu_{cmc}^{tri} = \mu_{cvc}^{tri} = \mu_{clc}^{tri} = \mu_{cmc}^{di}[1 + \rho(2^{11/6} - 1)]^{6/11} \qquad \text{(IV.3)}$$

As in the diblock copolymer case, the main contributions to the free energy result in identical critical chemical potentials; the degeneracy can only be resolved if corrective contributions from the elasticity of the chains in the core or the spontaneous curvature are taken into account. The contributions from the elasticity of the chains in the core can be calculated as in the diblock case. On general grounds we expect that the spontaneous curvature contributions to the free energy of the cylindrical phase is twice as large as that of the spherical phase. Thus, as far as compact core structures of B–A–B triblock copolymers are concerned, the phase formation of aggregates is similar to the phase formation for A–B diblock copolymers: the various parameters and phase boundaries are only shifted by numerical constants determined by the asymmetry of the two soluble blocks.

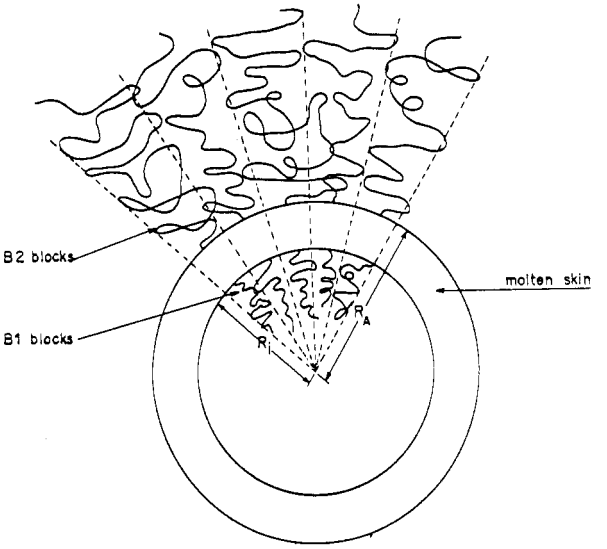

Figure 4. Geometry of a hollow structure in the case of triblock copolymers. We show the case of a micelle with generic asymmetry.

IV.2. Hollow Structures. B–A–B copolymers may also assemble as spherical and cylindrical structures where the collapsed A-blocks form a thin skin of molten polymers, protected by a double layer of swollen chains (see Figure 4). We can build these structures by a through experiment where we start from a planar symmetric layer and gradually reduce the number of monomers of the swollen blocks on one of its sides. Clearly the layer will bend to reduce the stretching energy of the larger chains, resulting in an optimal radius of curvature for the hollow structure.

In order to produce two asymmetric coronas, the A chains need to have each of their A–B connection points at opposite surfaces. In the *ball regime* this results in a high-energy penalty associated with the formation of curved structures (we recall that in this regime the elastic contribution from the A chains is dominant). In the opposite asymmetry limit, i.e., the *star regime*, the energy penalty to form near planar structures is very high so that double hair micelles are to be formed. The only regime where hollow structures might be found is the intermediate regime where the polymerization indices of both blocks B obey the inequality $N_{Bi}^{15/11} \ll N_A \ll N_{Bi}^{18/11}$ ($i = 1, 2$).

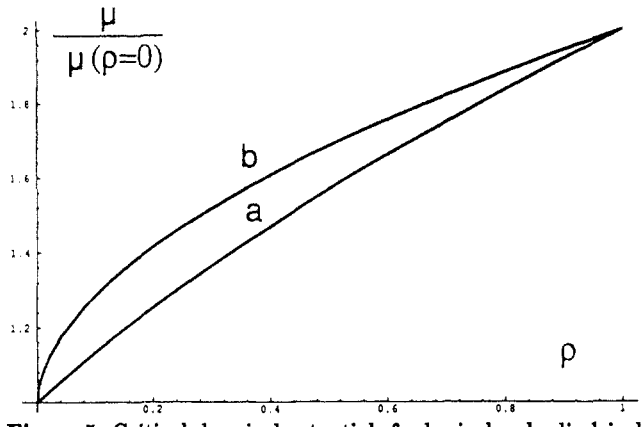

Figure 5. Critical chemical potential of spherical and cylindrical aggregates as a function of the asymmetry: (a) compact core structures; (b) hollow structures.

Let R_A be as above the external radius of the micelle and R_i its internal radius. These two radii are related to the aggregation number p by the incompressibility relation $pN_A = 4/3\pi(R_A^3 - R_i^3)$. The grand potential for the spherical hollow structures

$$\tilde{\Omega}_s = \frac{4\pi B}{3^{11/16}}r^{23/6}\left[1 + \frac{\rho}{\alpha^{5/3}}\right](1-\alpha^3)^{11/6} + 4\pi r^2(1+\alpha^2) - \tilde{\mu}\frac{4\pi}{3}r^3(1-\alpha^3) \quad \text{(IV.4)}$$

where we have set $\alpha = R_i/R_A$ and all quantities have been renormalized as in the corresponding diblock case. As before we minimize the grand potential with respect to the internal variables (r and α in this case) and obtain the critical chemical potential by setting the potential equal to zero. This leads to

$$\begin{cases} \mu_{cmc}^{tri} = \mu_{cmc}^{di}(1+\rho^{6/11}) \\ R_A^{tri} = R_A^{di}/(1-\rho^{9/11}) \\ \alpha = \rho^{3/11} \end{cases} \quad \text{(IV.5)}$$

A similar calculation for the cylindrical hollow structures gives

$$\begin{cases} \mu_{cyc}^{tri} = \mu_{cyc}^{di}(1+\rho^{6/11}) \\ R_A^{tri} = R_A^{di}/(1-\rho^{12/11}) \\ \alpha = \rho^{6/11} \end{cases} \quad \text{(IV.6)}$$

with the same renormalization factors. Equations IV.5 and IV.6 present similar features: identical chemical potentials and equilibrium external radii which tend (not surprisingly!) to infinity when $\rho \to 1$: lamellae are the equilibrium structures when both B-blocks have the same size. In Figure 5 we compare the stability of hollow and compact structures by sketching the corresponding critical chemical potentials as functions of the asymmetry (eqs IV.3, IV.5, and III.14). The figure shows that, at thermodynamic equilibrium, hollow structures are always unstable against compact core ones: they can only exist as metastable states. It is, however, important to stress that, if any hollow structure is formed out of equilibrium (for instance, by peeling out pieces of membranes which always exist close to the surface—a preparation method well-known for the formation of lipid vesicles), it can survive for a very long time in the metastable state, due to the very high potential barriers which separate the hollow from the compact structures.[10] Indeed, the mechanism of extracting a chain from a hollow structure involves an intermediate state where one of the B-blocks (say, the smallest) needs to cross the molten region of blocks B, leading to an energy barrier proportional to N_{B1}.

V. Conclusions

In this work we have studied the micellization of diblock and triblock copolymer chains in a selective solvent. We investigated the possible formation of dilute spherical or cylindrical phases and the appearance of dense lamellar phases. We find that, in the diblock copolymer case, only dilute spherical structures will be formed for $N_A \ll N_B^{3/2}$; above this limit, the dense lamellar structure is predicted to have the lowest chemical potential. Nevertheless, this does not rule out the existence of other dense geometries, a possibility that we hope to address in a forthcoming paper.

The micellization of triblock copolymer chains follows a similar scenario. However, an interesting new possibility may arise: due to the very long lifetime associated with polymeric micelles, metastable hollow structures may also be observed in the solution. This will, of course, depend crucially on the preparation method.

It is also worth noting that, for diblock copolymers in a selective solvent of high molecular weight (say, for instance, A–B diblock copolymers in a melt of large B homopolymers), there is a range of chemical composition for which the cylindrical phase is stable.[10] This raises another interesting issue related to the existence of a critical molecular weight of the solvent for which the cylinders cease to be thermodynamically stable.

Acknowledgment. We thank J. F. Joanny for helpful discussions. D.I. thanks Institut Charles Sadron (CNRS, U.P.R. 022) for their hospitality. The Brazilian fellowships CNPq and FAPESP are also fully acknowledged.

References and Notes

(1) Israelachvili, J. *Intermolecular and Surface Forces*, 2nd ed.; Academic Press: London, 1992.
(2) Leibler, L.; Orland, H.; Wheeler, J. *J. Chem. Phys.* **1983**, *29*, 3350. Halperin, A. *Macromolecules* **1987**, *20*, 2943. Zhulina, Ye. B.; Birshtein, T. M. *Polym. Sci. U.S.S.R.* **1985**, *27*, 570. Munch, M. R.; Gast, A. P. *Macromolecules* **1988**, *21*, 1360. Marques, C. M. Thèse présentée à l'Université Claude Bernard, Lyon I pour obtenir le titre de Docteur en Science.
(3) Johner, A.; Joanny, J. F. *Macromolecules* **1990**, *23*, 5299.
(4) Daoud, M.; Cotton, J. P. *J. Phys. (Fr.)* **1982**, *43*, 531.
(5) Witten, T. A.; Pincus, P. A. *Macromolecules* **1986**, *19*, 2509.
(6) Semenov, A. N. *Sov. Phys. JETP* **1985**, *61*, 733.
(7) *Statistical Mechanics of Surfaces and Membranes*; Nelson, D. R., Piran, T., Weinberg, S., Eds.; World Scientific: New York, 1989.
(8) Helfrich, W. *Z. Naturforsch.* **1978**, *33A*, 305.
(9) Shim, D. F. K.; Marques, C.; Cates, M. E. *Macromolecules* **1991**, *24*, 5309.
(10) Semenov, A. N. *Macromolecules* **1992**, *25*, 4967.